View metadata, citation and similar papers at core.ac.uk

brought to you by CORE

provided by NASA Technical Reports Server

D22 441

N82 26077

BROAD BAND X-RAY TELESCOPE (BBXRT)

P.J. Serlemitsos

Laboratory for High Energy Astrophysics

NASA/Goddard Space Flight Center

Greenbelt, MD 20771

ABSTRACT

An approach is presented along with corroborating measurements for significantly enehancing the potential of Si(Li) spectrophotometry in X-ray astronomy. The key new element is an unconventional X-ray mirror that meets qualifications of low cost, light weight, and large throughput over a broad energy band ($\gtrsim$ 7 keV) at moderate angular resolution. The potential for other applications is also discussed.

I. INTRODUCTION

I will be reporting on a 0.5-10 keV non-dispersive spectroscopy experiment proposed by the Goddard X-ray group some three years ago in response to NASA's Spacelab AO. It consists of 2 co-aligned grazing incidence telescopes with cooled Si(Li) spectrometers at each focus. BBXRT is a follow-up experiment to the solid state spectrometer contributed by the Goddard group and flown aboard the Einstein Observatory (experiment B-5; Joyce et al. 1978). It represents a major effort to tap new research areas that were not accessible with the previous instrument. Assigned to NASA's OSS-2

mission, it has been funded for definition and some limited hardware development. OSS-2 is not as yet on NASA's approved flight program. Some preliminary test results involving prototype telescope and detector hardware will be presented and discussed. We will also consider some specific observations from a shuttle mission that link the instrument's potential to several of the items that have surfaced in this meeting from the theoretical reviews as well as to potential goals of an explorer mission.

II. OBJECTIVES AND IMPLEMENTATION

BBXRT was conceived and is presently under development to meet the following objectives:

1. Expand the energy band of Si(Li) spectrophotometry to adequately include iron K-shell transitions.
2. Recover some measure of the spatial information that telescopes provide but which is lost in single-pixel photometry.
3. Reduce detector background sufficiently to make possible the study of the many new sources identified in Einstein IPC and HRI fields.

In spite of obvious limitations with resolution, focal plane Si(Li) spectroscopy has a potential that we have only begun to exploit with the instrument aboard Einstein. One direction to go for a predictably large impact on future observations is to extend the response of grazing incidence optics to about 10 keV. This would make possible the study of iron K-shell transitions which are the dominant transitions whether collisionally excited in hot plasmas with kT > a few keV or due to the fluorescence process. Even when the spectrum is featureless, a broad band-pass will result in better determination of the shape of the continuum and of any detectable absorption

effects at the low end of the spectrum.

Efficient reflection at the higher (~ 7 keV) energies will only occur from surfaces at small ($\lesssim$ 0.5 degrees) angles to the incident beam. In a cylindrical telescope geometry, the instrument focal length determines the maximum mirror aperture that satisfies the above condition. The high energy throughput will depend on how effectively we utilize the area within this limiting aperture. When nesting confocal surfaces it is imperative that we maximize the ratio of the reflecting to dead areas, the latter made up of mirror walls, gaps and supports.

The BBXRT mirror design opts for maximum high energy response at the expense of high resolution imaging. The latter is compromized by a drastic reduction in mirror wall thickness and by the use of an approximate geometry: both the paraboloid and the hyperboloid in the Wolter type I geometry are replaced with tightly nested confocal thin foil cones. Note that the approximation improves for small grazing angles and short cone segments. We have chosen a cone length which results in an intrinsic spatial resolution < 0.5 arc minute half power radius (i.e. if we neglect mirror distorsions and assembly tolerances). The foil reflectors are formed from .005-inch, high quality but commercially available aluminum foil overcoated with ~ 10μ of acryllic lacquer on which ~ 500 $\mathring{A}$ of gold is vacuum deposited. This simple surface preparation replaces the customary polishing which, aside from cost, would be quite impratical in this case. As we shall show, it produces a surface smoothness comparable with that of highly polished surfaces.

The parameters for each of the 2 BBXRT mirrors are listed in Table 1. Note in particular that the efficiency for utilizing the telescope aperture is 0.7 (0.6 if the small central void is added to the dead area) which is not too different from the transmission efficiency of the collimation to a large area

gas proportional counter. In Figure 1 we have plotted the net geometric area for each mirror as a function of the angle for an off-axis incident beam. We wish to point out that as the effective area is reduced due to vignetting, the image quality is independent of off-axis position for this type of geometry.

We have used the 150 ft long X-ray calibration facility at Goddard to calibrate a telescope segment (quadrant) equipped with only the inner most 50 reflectors due to beam size limitations. This segment is shown in Figure 2. The beam divergence results in considerable vignetting which was taken into consideration when computing the reflection efficiency. Furthermore, it increases the grazing angles at the front mirror by about 30% which would tend to reduce the measured response at high energies. We have not corrected for this effect. Figure 3 shows the measured response for the 50 reflector complement of the BBXRT mirror (net geometric area 220 cm^2) using bremsstrahlung off a beryllium target intercepting a 20 keV electron beam as well as characteristic lines from the various other targets listed on the figure. We used at the focus a cooled Si(Li) detector ~ 6 arc minutes in radius. Our measurements did not extend below ~ 1.2 keV because of a beryllium detector cover. Reflection efficiencies inferred from these results are in good agreement with those compiled by Seward (1977) for gold-coated mechanically polished mirrors. Assuming that this agreement holds for the entire range of grazing angles of the full telescope complement we have estimated the combined effective area of the 2 BBXRT telescopes as shown in Figure 4. For a rough comparison, we have included in the figure the measured response of the Einstein solid state spectrometer.

We have not as yet been able to fully evaluate the imaging potential of this telescope. Ray tracing indicates that the approximate geometry yields images with < 0.5 arc minutes half power radius (HPR). Aside from the

geometry however, the image quality will depend on other factors as well such as distortions of the foil reflectors whether inherent in the foil or introduced in the assembly process and, possibly, surface roughness. Preliminary results from our calibration of the prototype telescope segment indicate an image with ~ 3 arc minutes HPR independent of energy. This energy independence rules out surface roughness as the major cause of image broadening. Other evidence seems to indicate that errors in the reflector assembly may be mostly responsible for the observed degraded image. A goal of ~ 2 arc minutes HPR, consistent with the size of the BBXRT detectors, should be achievable.

Coming next to our second objective of recovering some of the spatial information while still maintaining the Si(Li) energy resolution, we have developed a 5-element Si(Li) detector specifically for this application by segmenting a single silicon crystal as shown in Figure 5. At the focus of the BBXRT mirror, the central element extends to 3.7 arc minutes radius whereas the outer pixel perimeter is at 8.6 arc minutes. The partitioning grooves are 0.5 arc minutes wide. This type of detector allows the study of isolated weak point sources while simultaneously monitoring background in adjacent pixels. For diffuse sources with several arc minutes extent it increases the efficiency for generating rough spectral maps. In preliminary tests we find identical performance for all pixels with an energy resolution comparable to that of the Einstein instrument.

Our third objective stems from the fact that virtually nothing is known about the X-ray spectra of sources at flux levels $\lesssim 10^{-11}$ ergs $cm^{-2}s^{-1}$. The sample includes the majority of the new sources discovered with the imaging detectors aboard the Einstein observatory from stars to distant clusters of galaxies and quasars. What prevented the Si(Li) spectrometer aboard Einstein

from supplying some of this information was a high background rate totally unrelated to the telescope throughput.

Background reduction schemes relevant to this instrument must necessarily deal with the radiation environment and its effects as contrasted, for example, with reducing the size of pixels. Background events may result from direct interactions in the detector sensitive volume, intercations near the detector edges resulting in partial charge collection, electronic cross talk from large events in the outer unused detector perimeter, enhanced noise associated with electronic baseline distortions caused by large ionizing events, etc. The 5-pixel detector offers us the opportunity to apply pixel-to-pixel anticoincidence which is a proven technique for eliminating a large fraction of the above-mentioned background. In addition, we have incorporated a charged particle guard in the form of a CsI(Tℓ) cup placed around the detector and its cold finger assembly as shown in Figure 6. The size of this cup and, therefore, the cost and complexity associated with it have been kept to a minimum by the use of a cooled Si(Li) detector for detecting the light pulses from the CsI. The detector views the CsI without coupling through a port at the inner surface of the base of the crystal. The threshold for anticoincidence is set at ∿ 300 keV, well below the ionization losses of singly charged minimum ionizing particles. Although this relatively small crystal would not be very effective in actively guarding the detector from γ-rays as well, the 0.5 inch high-Z walls form an efficient passive shield up to γ-ray energies of ∿ 200 keV.

We have completed an initial evaluation of the BBXRT detector background using a prototype cryostat assembled in the manner shown in Figure 6. This was done in an enhanced radiation environment from a Co^{60} source as well as at ambient ground level (no source) conditions. We did confirm that, at ground

level, the dominant background reduction scheme is the pixel-to-pixel anticoincidence rather than the CsI guard. Figure 7 shows the background reduction effected when the Co^{60} source was in the proximity of the cryostat. Note the relatively small improvement obtained near the threshold energy of 0.5 keV as compared with the substantial gains at higher energies.

Ground level detector performance in the absence of sources is significant in that it is often a reliable measure of the performance to be expected in space: in the few keV range, gas proportional counters flown by our group displayed in space a background rate typically within a factor of ~ 2 of their ground level background. In Table 2 we have tabulated the observed BBXRT ground level background along with a measure of the gain realized in a direct comparison to solid state spectrometer aboard Einstein. Again we point out the relatively modest improvement at the lower energies in rough agreement with the Co^{60} results.

In summary, we have demonstrated that the background reduction techniques we have incorporated result in substantial gains especially at energies > 1 keV. It is apparent that some additional effects dominate the background rate at the very low energies and these have to be dealt separately.

III. OBSERVATIONS FROM THE SPACE SHUTTLE

BBXRT is well suited to carrying out observations with typical exposures of a few x 10^3 s as would be the case with a ~ 7 day shuttle mission. With regard to extragalactic objects we may single out quasars and clusters of galaxies as the two classes of sources where substantial gains could be made with this instrument. In Table 3 we indicate what could be a typical example involving a quasar with a spectrum as in 3C273 (Worrall et al. 1979) at a flux

level of 10^{-12} ergs cm^{-2} s^{-1}. For our field of view, source confusion would not generally come into play for at least one order of magnitude below this sensitivity. We have assumed a 2-fold increase in instrument background over what was measured at ground level. We note that such an observation would be essentially photon limited over most of the spectral range and that a 2000 s exposure would be quite adequate for deducing the shape of the spectrum for such an object.

Similar arguments apply to the sensitivity for measuring the spectral shape and, therefore, the temperature of distant clusters of galaxies. On the other hand, the possible detection of Fe lines from these sources from which other parameters such as the redshift may be inferred is considerably more demanding. BBXRT will have typically 200 eV FWHM resolution at 7 keV. In a 2000 s observation the prominant Fe line blend from a Perseus-like cluster at $Z \approx .2$ will be detected at the 3σ level. For the nearby clusters it will be possible to make accurate Fe abundance determinations and to search for possible temperature and Fe abundance grandients with distance from the cluster center. For the Virgo cluster we will be studying the emission associated with individual galaxies such as M86. An observational program will, of course, include other classes of extragalactic sources as well. The two-component spectra of BL Lac objects and the large column densities and iron absorption edges associated with some of the Seyferts are spectral characteristics that can best be studied with this broad-band instrument.

Potentially interesting observations of galactic sources will include the temperature classification of the various types of stars. Iron line equivalent widths should help us determine the nature of the high energy component associated with some systems such as the RS CVn binaries (Swank et al. 1981). Iron line emission and absorption features invariably appear in

the spectra of the more luminous binaries and X-ray pulsars (Pravdo 1978). The type of questions that could be answered with this instrument deal with line broadening, multiple components, Doppler shifts, fluorescence, phase dependence, etc. Spectra of supernova remnants obtained with the Einstein instrument are rich in line features (Becker et al. 1980). The addition of the higher energy lines and continuum should help separate non-equilibrium effects from bonafide abundance anomalies.

IV. FUTURE PROSPECTS

We believe that all aspects of the experiment we have described may well have a bearing on a future Explorer mission. We have demonstrated the feasibility of segmenting a large Si(Li) detector into smaller elements for focal plane use. We have also outlined techniques for suppressing the background for such an array in order to make it effective in the study of weak sources. However we view as the single most important contribution the radically new way of realizing a broad-band, large throughput instrument at moderate angular resolution. Key elements are a simple reflector surface preparation and an approximate telescope geometry which greatly simplifies reflector preparation and assembly. The fabrication of such a telescope is actually not too different from what is involved in the assembly of a large area gas proportional counter. To the extent that large throughput at low cost is a necessary ingredient of a future Explorer mission, we believe that our approach deserves serious consideration. For example we can achieve 10^4 cm^2 of effective area in 16 modules inside a 2 M envelope. The corresponding area at 7 keV would be $\bullet$ 1600 cm^2.

The BBXRT spatial resolution is probably inadequate for an Explorer

instrument although it suffices for the instrument we are developing. We wish to emphasize that the cause of the broader image does not lie in the approximate geometry. It is quite conceivable that even with the thin foil reflectors we are using we could eventually improve on our image quality through better reflector preparation and assembly. If not, it would be a matter of seeking a better balance between throughput and reflector thickness. The potential for 0.5 arc minute HPR image is simply there.

I wish to acknowledge major contributions to this project by C. Glasser, F. Birsa and D. Arbogast.

REFERENCES

Becker, R.H., Holt, S.S., Smith, B.W., White, N.E., Boldt, E.A., Mushotzky, R.F., and Serlemitsos, P.J. 1980, Ap. J. (Letters) 235, L5.

Joyce, R.M., Becker, R.H., Birsa, F.B., Holt, S.S., and Noordzy, M.P. 1978, IEEE Trans. Nuc. Sci 25, 453.

Pravdo, S.H. 1978, Proceedings of the XXI COSPAR/IAU Symposium in X-Ray Astronomy, Pergamon Press, Ltd., Oxford.

Seward, F.D. 1977, Lawrence Livermore Lab., UCID-17505.

Swank, J.H., White, N.E., Holt, S.S., and Becker, R.H. 1981, Ap. J. 246, 208.

Worrall, D.M., Mushotzky, R.F., Boldt, E.A., Holt, S.S., and Serlemimtsos, P.J. 1979, Ap. J. 232, 683.

TABLE 1

BBXRT TELESCOPE PARAMETERS

Max (Min) Dia.	43 (17.8) cm^2
Focal Length	3.8 M
Focal Plane Scale	0.91 arc min/mm
Spatial Resolution	
Intrinsic	< 0.5 arc min HPR
Goal	2 arc min HPR
Mirror Material	.005 inch Al foil (Gold)
Number of Nested Mirrors	101 (4-inch cones)
Grazing Angles	0.34 - 0.75 deg
Aperture Utilization	0.6
Weight	10 kg

TABLE 2

BBXRT PROTOTYPE GROUND LEVEL DETECTOR BACKGROUND

E(keV)	COUNTS s^{-1} keV^{-1}	GAIN OVER SSS
.5 - 1.0	2.3×10^{-2}	9
1.0 - 1.5	4.1×10^{-3}	20
1.5 - 2.0	1.8×10^{-3}	33
2.0 - 3.0	5.4×10^{-4}	89
3.0 - 11.0	2.4×10^{-4}	--

TABLE 3

QUASAR SPECTRA; 2000 s EXPOSURE
EXPECTED COUNTS

	ENERGY BINS (keV)		
	1-2(1000 cm^2)	3-4(450)	6-7(200)
3C273* $dN/dE = .022E^{-1.55}$ $N_H < 2.2 \times 10^{21}$ cm^{-2}	> 19700	2820	484
Same spectrum renormalized to 10^{-12} ergs/cm^2s (2-10 keV)	> 180	25	4.4
Diffuse Background	17.4	2.4	0.4
Detector Background	24	2	2

*Worrall et al. 1979

ORIGINAL PAGE IS
OF POOR QUALITY

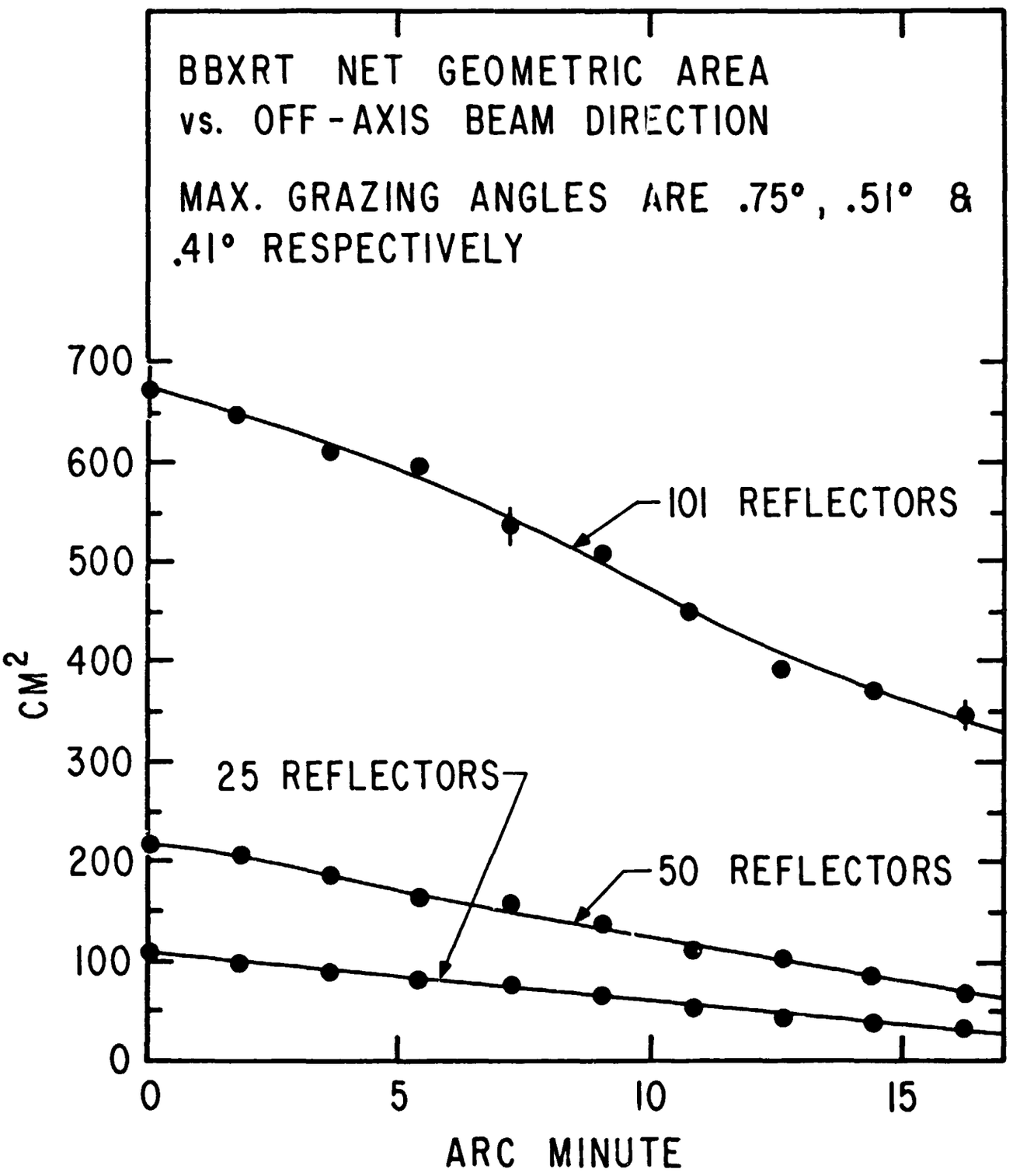

Figure 1

ORIGINAL PAGE
BLACK AND WHITE PHOTOGRAPH

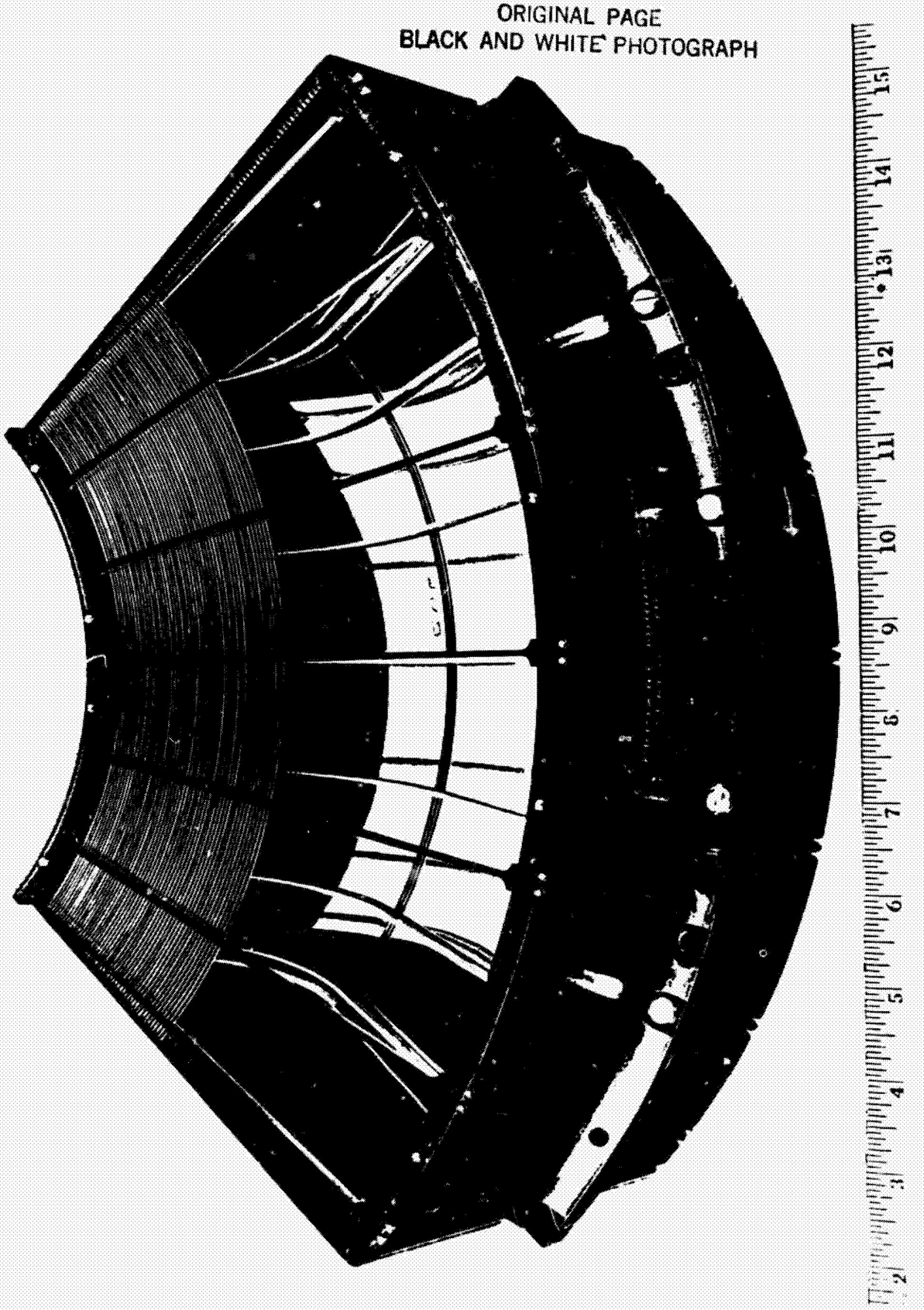

Figure 2

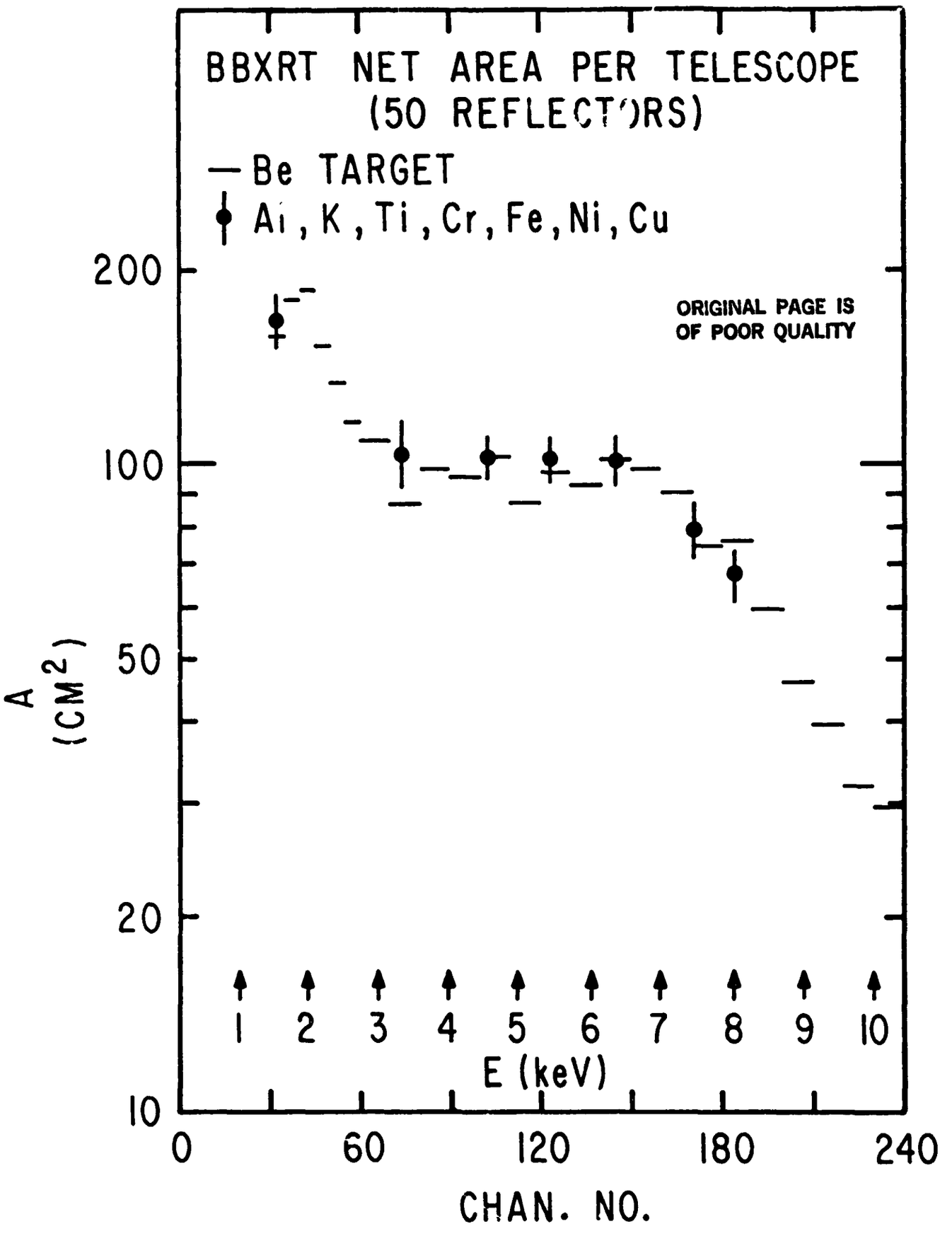
BBXRT NET AREA PER TELESCOPE
(50 REFLECTORS)
— Be TARGET
Al, K, Ti, Cr, Fe, Ni, Cu
ORIGINAL PAGE IS
OF POOR QUALITY
200
100
50
20
10
A
(CM²)
1 2 3 4 5 6 7 8 9 10
E (keV)
0
60
120
180
240
CHAN. NO.

Figure 3

ORIGINAL PAGE IS
OF POOR QUALITY

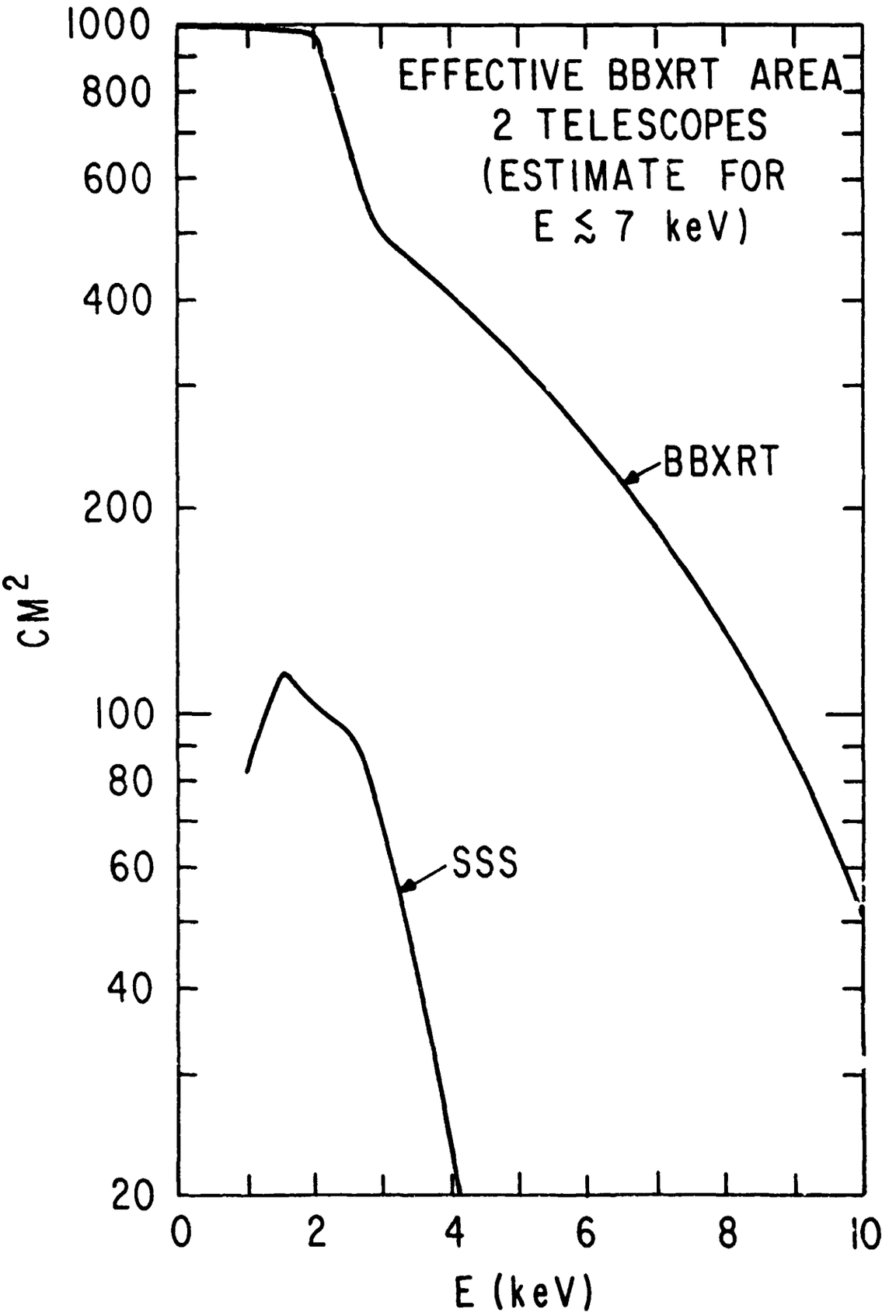

Figure 4

ORIGINAL PAGE IS
OF POOR QUALITY

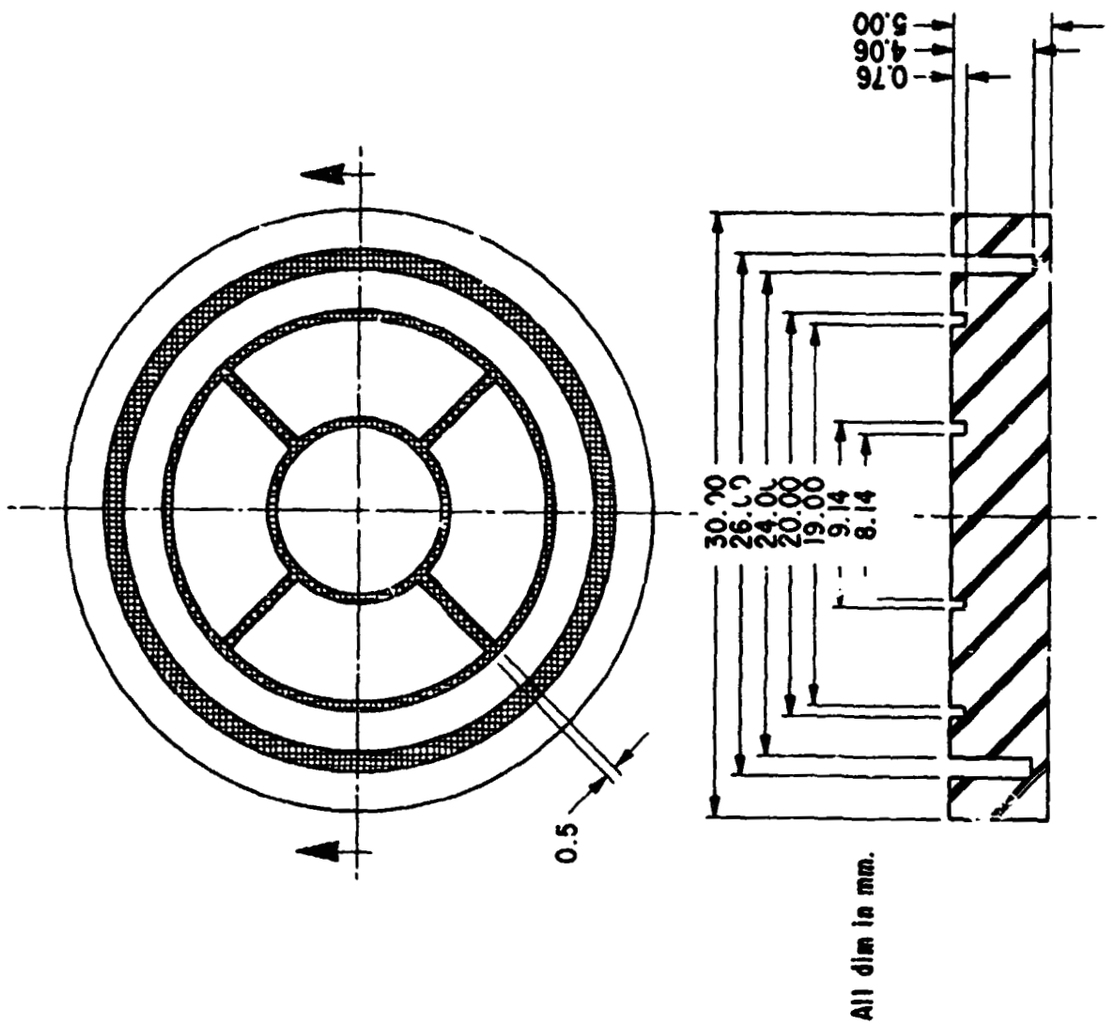

Figure 5

ORIGINAL PAGE IS
OF POOR QUALITY

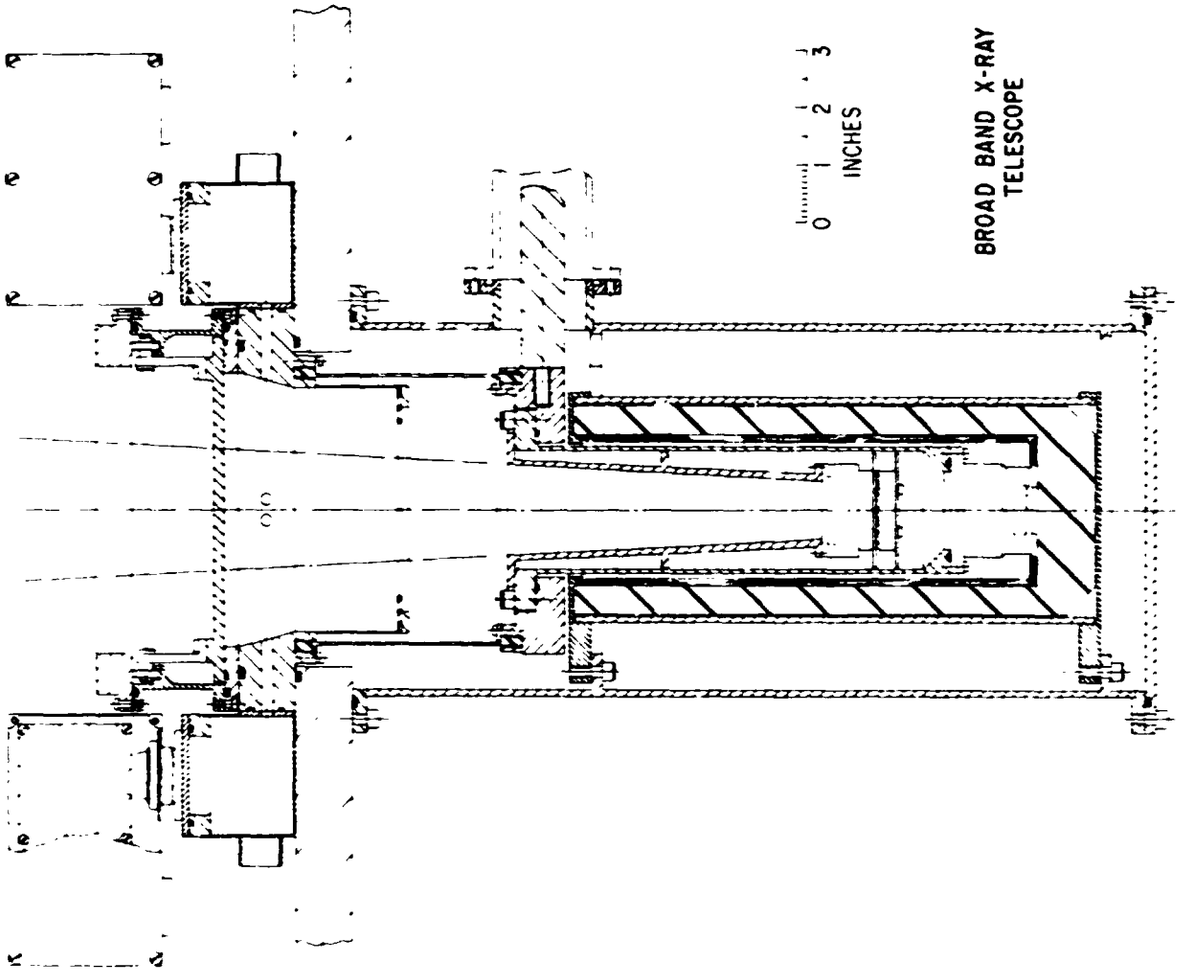

F gure o

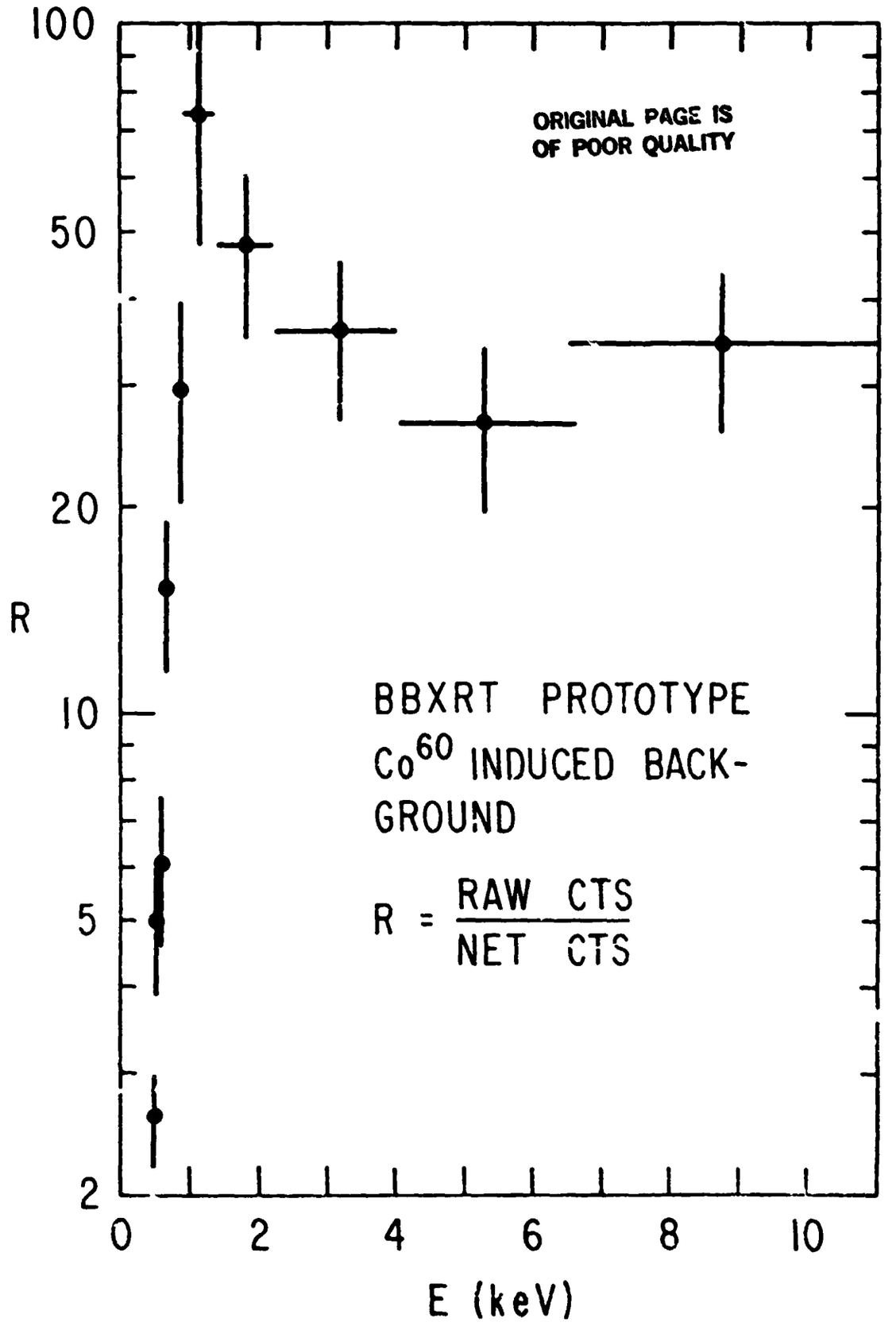
100
50
20
10
5
2
R
0
2
4
6
8
10
E (keV)
ORIGINAL PAGE IS
OF POOR QUALITY
BBXRT PROTOTYPE
Co60 INDUCED BACK-
GROUND
R = RAW CTS / NET CTS

Figure 7